

Hepatocyte culture in a radial-flow bioreactor with plasma polypyrrole coated scaffolds

ODIN RAMÍREZ-FERNÁNDEZ^{1*}, RAFAEL GODÍNEZ¹, ESMERALDA ZUÑIGA-AGUILAR¹, LUIS E. GÓMEZ-QUIROZ², MARÍA C. GUTIÉRREZ-RUIZ², JUAN MORALES³, ROBERTO OLAYO³

¹ Departamento de Ingeniería Eléctrica, Universidad Autónoma Metropolitana, Unidad Iztapalapa, Apdo. Postal 55-534, Iztapalapa, México.

² Departamento de Ciencias de la Salud, Universidad Autónoma Metropolitana, Unidad Iztapalapa, Apdo. Postal 55-534, Iztapalapa, México.

³ Departamento de Física, Universidad Autónoma Metropolitana, Unidad Iztapalapa, Apdo. Postal 55-534, Iztapalapa, México.

Key words: Cell Cultures, Flow Simulation, Flow Features, HepG2 Cells, Plasma Polymerization.

ABSTRACT: We have designed and evaluated a radial-flow bioreactor for three-dimensional liver carcinoma cell culture on a new porous coated scaffold. We designed a culture chamber where a radial flow of culture medium was continuously delivered through it. Once this system was established, flow was simulated using flow dynamics software based on numeric methods to solve Navier-Stokes flow equations. Perfusion within cell culture scaffolds was simulated using a flow velocity of 7 mL/min and found that cell culture medium was distributed unhindered in the bioreactor chamber. Afterwards, the bioreactor was built according to the simulated design and was tested with liver carcinoma cells (HepG2) cultured over an L-poly(lactic acid) scaffold whose surface was modified with iodine-doped polypyrrole. The bioreactor was tested under non-flow and in radial flow conditions. Cell density under radial flow conditions was almost double than that under static conditions and both total protein and albumin output was also increased under radial flow conditions.

Introduction

Bioartificial livers (BAL) are based on hepatocytes cultured within a bioreactor and are intended to obtain an efficient temporal therapy for acute hepatic failure (Biederman *et al.* 2000, Carpentier *et al.* 2009). BALs utilize cultured hepatocytes within a device providing artificial flow so that plasma and blood from a patient can exchange substances with hepatocytes within the bioreactor, through a semipermeable membrane in order to detox patient blood, in a way that the liver damaged can still secrete important metabolites (Carpentier *et al.* 2009).

A suitable environment is required to mimic the physiological structure of liver tissue (Carpentier *et al.* 2009, Chen *et al.* 2008). Conventional hepatocyte cultures are made on

a bidimensional surface and without nutrients flow. These static cultures are subject to local changes in culture medium degradation, pH, accumulation of excretory metabolites, etc., while bioreactors are intended to obtain tridimensional cell cultures, with a better distribution of nutrients, thus enhancing metabolic production and cell growth (Chen *et al.* 2008, Du *et al.* 2008). Tissue engineering has also attempted to develop bioreactors in which tridimensional cultures will eventually organize as a fully functional tissue, thus approximating the *in vivo* conditions (Freshney 2009, Galbusera *et al.* 2007).

Radial flow bioreactors (RFBs) may solve many of the problems found using conventional artificial liver systems. This is achieved through the use of an extended cylindrical bed matrix made of porous bead microcarriers and a medium flowing continuously from the periphery towards the central axis (Li *et al.* 2009). This kind of systems supports high density, large scale cell cultures with long-term viability (Kosuge *et al.* 2007, Miyazawa *et al.* 2007) based on the

*Address correspondence to: Odin Ramírez-Fernández,
odinramirezfernandez@gmail.com

Received: June 26, 2014 Revised version received: August 3, 2015

Accepted: August 15, 2015

beneficial concentration gradient of gases and nutrients produced by a continuous flow through the matrix, which also prevents shear stress or buildup of waste products.

The design of a bioreactor must consider the hydrodynamic features to meet the flow conditions of the liver tissue (Li *et al.* 2009). Computational flow dynamics (CFD) is an important tool used for tissue engineering that helps to define the system hydrodynamics in the presence of cellular scaffolds (McKenzie *et al.* 2008). Bioreactor design is based on the scaffold hydrodynamic insight analysis and some of the controllable variables, such as scaffold morphology (pore size, fiber diameter, etc.) and initial cell distribution. These variables are used to solve Navier-Stokes flow equations to define speed in the bioreactor field lines and to approximate both the scaffold and the bioreactor performance (Li *et al.* 2009, McKenzie *et al.* 2008, Morales *et al.* 2008, Park *et al.* 2005, Park *et al.* 2008).

Poly(lactic acid) (PLLA) is a widely used biomaterial for scaffold construction, whose surface can be easily modified to improve its adhesion properties (Ramirez-Fernandez *et al.* 2012, Sherman 2005, Shi *et al.* 2004, Shoufeng *et al.* 2001). Plasma polymerized pyrrole (Ppy) modified PLLA surfaces have shown improved cellular adhesion and increased proliferation and life span of cell cultures (Thomas *et al.* 2006, Wang *et al.* 2004, Zhang *et al.* 2001).

We here present the design, construction and validation of a radial flow bioreactor in which cells from a human hepatocellular carcinoma (HepG2 line) were cultured on iodine-doped polypyrrole (Ppy-I) coated PLLA scaffolds. Such bioreactors may prove useful to build BALs for patients suffering acute hepatic insufficiency.

Materials and Methods

System description

The RFB (Fig. 1) consists of a cylindrical glass recipient (50 mm x 100 mm) bearing a food-grade stainless steel central

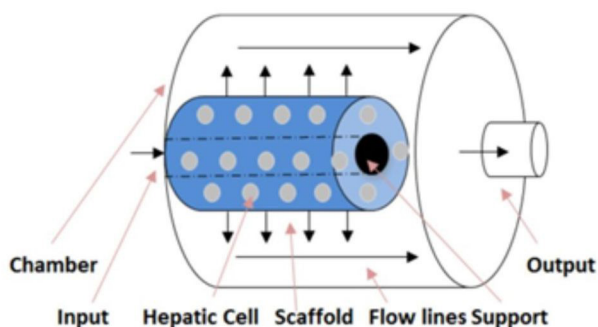


FIGURE 1. Outline of the radial flow bioreactor (RFB).

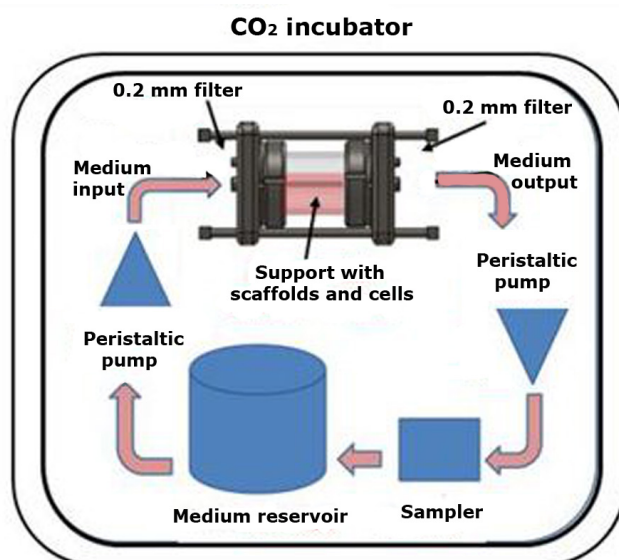


FIGURE 2. System design.

bracket (T-304, diameter 6.35 mm) with 1mm drills distributed all over the surface so that the cell-bearing scaffold (60 mm x 25 mm x 5mm) can be placed before filling the chamber with medium at 80% of its storage capacity, and placing it in a temperature regulated, 5%CO₂ incubator (Fig. 2). Two peristaltic pumps drive the culture medium through the chamber and across the scaffold's metal bracket (Fig. 2). Gases diffuse into the chamber across the 0.2 μm filters. The hoses (6.35mm diameter) connecting the peristaltic pumps and the sampler are made of medical-grade PVC.

Model design

Data from flow simulation may assist the calculations to avoid zero flow zones within the bioreactor. Hence, a geometrical bioreactor model was designed at SolidWorks (Systems Dessault, inc.). The model was then exported to CosmosFlowworks (Systems Dessault, inc.) software to solve Navier-Stokes equations to determine speed fields and work against the scaffold. The physical culture features were: isothermal, Newtonian liquid, 1,000 kg/cm³ density, 0.889mPa viscosity and 7 mL/min continuous flow. For the scaffold a 500 μm pores polyethylene sponge was used, together with Pyrex-type glass and stainless steel (T-304) metallic parts.

Surface-modified scaffold

PLLA sponges were 25-100 mg/cc density and 90% porosity (BIOFELT®, Concordia Fibers; Concordia Manufacturing Corp., Inc., Coventry, RI, USA) and their surfaces were modified with iodine-doped polypyrrole (Ppy-I). Plasma discharge was at 9×10^{-2} Torr pressure (Morales *et al.* 2008), measured with a Pirani valve (Edwards Vacuum, Inc., Sonora MX; 50 watts, 13.5 MHz). Pyrrole monomers were used

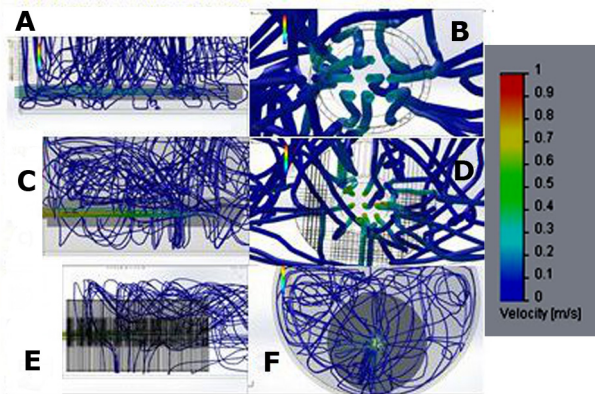


FIGURE 3. Colorimetric plot of velocity field and shear stress levels for different thickness of the scaffold. Panels A, C and E show lateral views for 0.5 cm, 10 cm and 5 cm, respectively. Panels B, D, and F show corresponding frontal views.

(98%, Sigma-Aldrich) and iodine (98%, Sigma-Aldrich). Monomers feeding was alternated in an iodine-pyrrole sequence for 4 min, only pyrrole for 6 min, iodine-pyrrole for 4 min and pyrrole for 6 min. Twenty min was the total reaction time.

Cell culture

HepG2 cell line (ATCC HB8065) was obtained from the American Type Culture Collection and were cultured as a monolayer with type E Williams culture medium (Gibco 12551) supplemented with 10% fetal bovine serum (Gibco 16000), 100 units/mL penicillin and 100 mg/mL streptomycin. Cells were cultured in flasks (Nunc, EE.UU.), 5% humidity, 5% CO₂, 95% air, and the culture medium was replaced twice weekly. Cells were trypsinized and cultured again every 7 days.

Cell density was measured at the time of seeding and after 15 days culturing in the RFB with 80 mL medium, both at zero flow and at 7 mL/min constant flow.

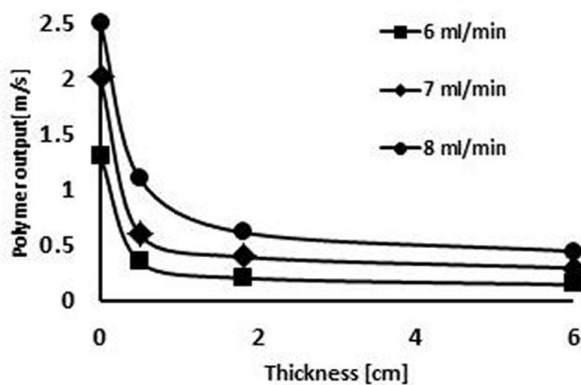


FIGURE 4. Radial velocities on the external surface of the scaffold at different input velocities.

Protein quantification

Total protein concentration in the outflow was measured from days 9 to 15, using the bicinchoninic acid kit (BCA, ThermoScientific; cat. 23255) using bovine serum albumin as standard; 0.5 mL supernatant samples were obtained daily and measured in a multimodal DTX 880 detector (BeckmanCoulter). Triplicate measures were obtained.

Albumin quantification

Elisa test was used to quantify albumin secretion into the supernatant from days 10 to 15 (AssayproEA2201-1); 0.5 mL supernatant samples were obtained daily and measured in a multimodal DTX 880 detector (BeckmanCoulter). Triplicate measures were obtained.

Data analysis

Data are presented as means (± SEM) of at least three independent experiments. Multiple comparisons were made using ANOVA followed by the Tukey test, using Origin 8.1 software. A P value of less than <0.05 was considered significant.



FIGURE 5. A. Bioreactor. B. Bioreactor connected to the peristaltic pump with culture medium (80 ml). C. Bioreactor with culture medium and PLLA scaffold. D. Bioreactor installed within the CO₂ incubator.

Results

Functional simulation of the RFB is shown in Fig. 3 with three different scaffold thicknesses, in both frontal and lateral views. Initially there is a speed gradient inside the central bracket, but speed stabilizes afterwards (lateral views, Fig. 3A, C and E); frontal views show a suction vortex at the RFB exit, and no static zones are observed. Simulations showed that radial flow through the scaffold is independent of scaffold thickness as we can see in the images with velocities of 2m/s in the inlet, 0,6 m/s across the scaffold and 0,2 m/s in the interchange chamber.

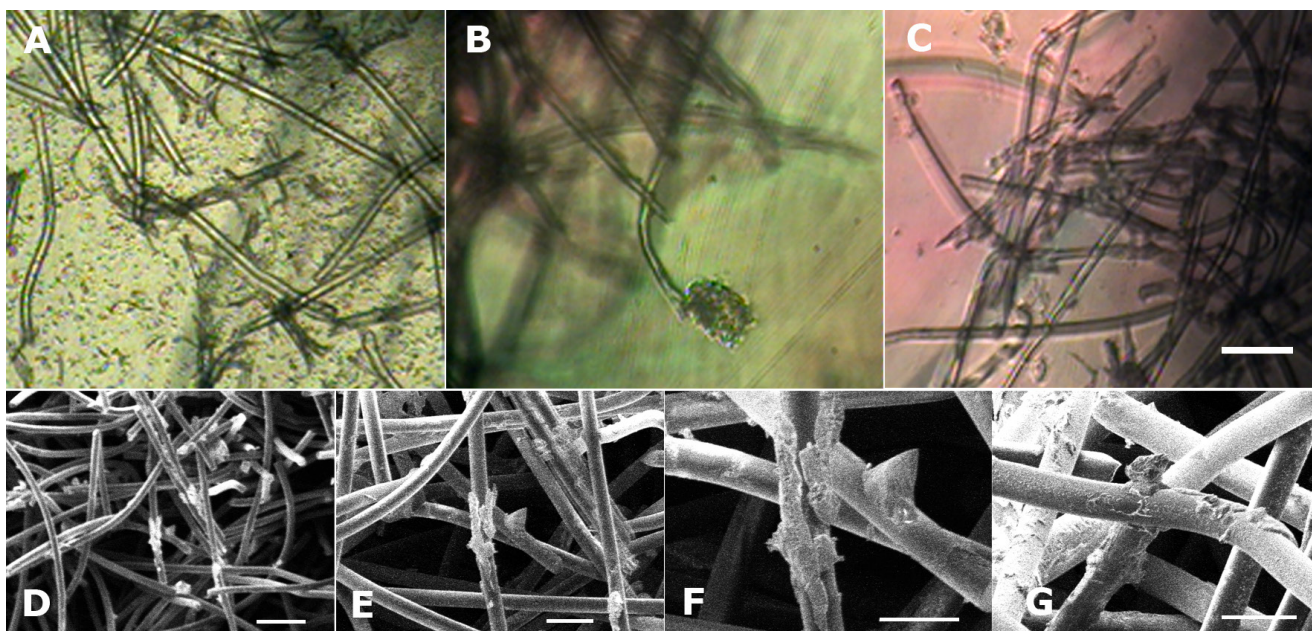


FIGURE 6. A, B and C show different zones of a 15 days non-flow culture under light microscopy; scale bar represents 50 μm . D, E, F and G show different zones of the same culture under scanning electron microscopy.

Flow rates cover a wide range of magnitudes in the simulation. However, under equal fluid inlet conditions field velocity decreased when the scaffold thickness increased as 0.6 m/s for 0.5 cm, 0.4 m/s for 1.8 cm and 0.3 m/s for 6 cm; but flow was always maintained perpendicular to the seeded cells. According to this, we can effectively reduce shear stress by choosing appropriate materials, geometry and location, even when the flow rate does not change.

Then we generated characterization curves for scaffold velocity (Fig. 4), that can describe the system response when the medium velocity and the scaffold thickness vary. Those curves gave us an idea of the optimal values that do not generate a high shear stress or a low medium flow.

We then proceeded to the RFB construction (Fig. 5) which was based on the simulation data. The steel RFB parts were processed by a computerized numeric control (CNC) machine.

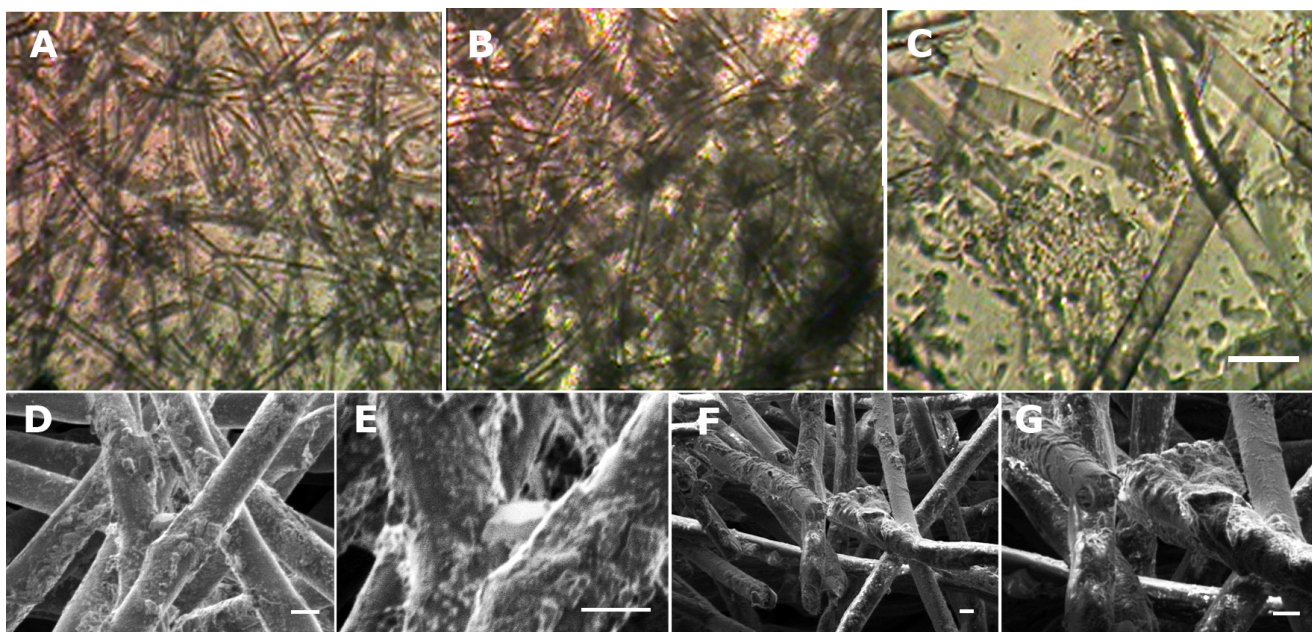


FIGURE 7. A, B and C show different zones of a 15 days culture at 7 mL/min radial flow conditions; light microscopy, scale bar represents 50 μm . D, E, F and G show different zones of the same culture under scanning electron microscopy.

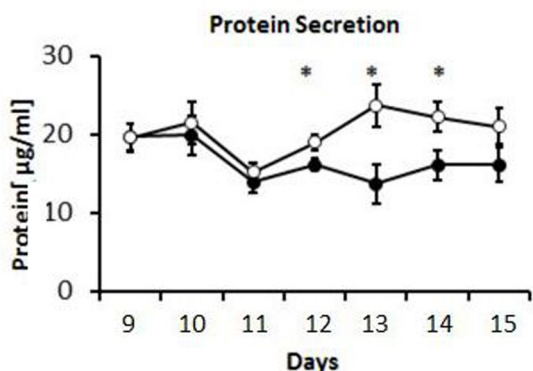


FIGURE 8. Protein secretion as a function of time. Black circles indicate static cultures, and white circles indicate radial flow cultures. Stars indicate statistically significant differences ($P < 0.05$; Student's t test).

Light and scanning electronic microscopy pictures of the cultures with zero flow or with 7 mL/min flow are shown in Figs. 6 and 7, respectively. Cells were attached to the scaffold fibers in both conditions, but more cells were covering the scaffold and were forming cell aggregates under the 7 mL/min flow conditions (Fig. 7).

Fig. 7 also shows the cellular distribution on the Ppy-I scaffold, where cell aggregates are visible around the fibers. This distribution is characteristic of high proliferative rate. The SEM images on Fig. 7 show a continuous cell layer around the fibers, indicative of an adequate adhesion of cells to Ppy-I surface modified fibers.

Cell density under radial flow conditions was almost double than that under static conditions (9.10×10^5 cells/mL and 5.38×10^5 cells/mL, respectively). Total protein (Fig. 8) and albumin (Fig. 9) production was also increased under radial flow conditions.

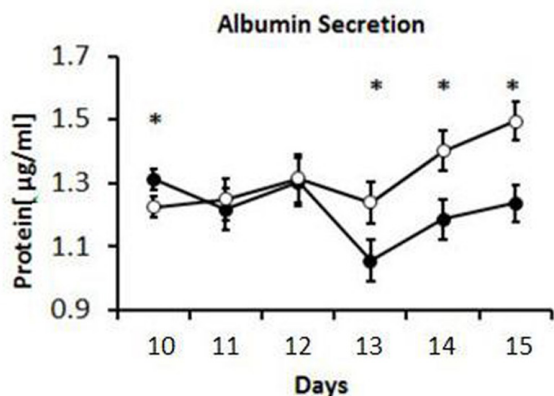


FIGURE 9. Albumin secretion as a function of time. Black circles indicate static cultures, and white circles indicate radial flow cultures. Stars indicate statistically significant differences ($P < 0.05$; Student's t test).

Conclusions

A RFB was designed and built in which the scaffold materials and pore size may be changed while maintaining the flow features and the radial distribution of the culture medium. Three-dimensional cell cultures could be obtained on surface modified PLLA fibers coated with Ppy (Ramirez-Fernandez *et al.* 2012).

The characterization curves described for the RFB model and the velocity vectors may be used to predict optimal scaffold volume and culture medium velocity for high density cell cultures which result in better total protein and albumin outputs. These approaches may result in better BALs performances.

Acknowledgements

The authors thank Universidad Autónoma Metropolitana (UAM), Consejo Nacional de Ciencia y Tecnología (CONACYT) (project 155239) and Instituto de Ciencia y Tecnología del Distrito Federal (ICyT-DF) (PIUTE 10-63276/2010) y (PICSA 11-14/2011) for funding.

References

Biederman H, Slavinska D (2000). Plasma polymer films and their future prospects. *Surface and Coatings Technology* **125**: 371- 376.

Carpentier B, Gautier A, Legallais C (2009). Artificial and bioartificial liver devices: present and future. *Gut* **58**: 1690-1702.

Chen XB, Li M G, Ke H (2008). Modeling of the Flow Rate in the Dispensing-Based process for Fabricating Tissue Scaffolds. *Journal of Manufacturing Science and Engineering* **130**: 210031-210037.

Du Y, Han R, Wen F, San San SN, Xia L, Wohland T, Leo HL, Yu H (2008). *Synthetic sandwich culture of 3D hepatocyte monolayer. Biomaterials* **29**: 290-301.

Freshney RI, (2009). *Culture of Animal Cells, a Manual of Basic Technique*, (John Wiley & Sons ed.), p. 150-184.

Galbusera F, Cioffi M, Raimondi M, Pietrabissa R (2007). Computational modeling of combined cell population dynamics and oxygen transport in engineered tissue subject to interstitial perfusion. *Computer Methods in Biomechanics and Biomedical Engineering* **10**: 279-287.

Ishii Y, Saito R, Marushima H, Ito R, Sakamoto T, Yanaga K (2008). Hepatic reconstruction from fetal porcine liver cells using a radial flow bioreactor. *World Journal of Gastroenterology* **14**: 2740-2747.

Kosuge M, Takizawa H, Maehashi H, Matsuura T, Matsufuji S (2007). A comprehensive gene expression analysis of human hepatocellular carcinoma cell lines as components of a bioartificial liver using a radial flow bioreactor. *Liver International* **27**: 101-108.

Li MG, Tian XY, Chen XB (2009). Modeling of Flow Rate, Pore Size, and Porosity for the Dispensing-Based Tissue Scaffolds Fabrication. *Journal of Manufacturing Science and Engineering* **131**: 034501.

Li MG, Tian XY, Chen XB (2009). A brief review of dispensing-based rapid prototyping techniques in tissue scaffold fabrication: role of modeling on scaffold properties prediction. *Biofabrication* **1**: 032001.

- McKenzie T, Lillegard JB, Nyberg SL (2008). Artificial and Bioartificial Liver Support. *Seminars in Liver Disease* **28**: 210-217.
- Miyazawa M, Torii T, Toshimitsu Y, Okada K, Koyama I (2007). Hepatocyte dynamics in a three-dimensional rotating bioreactor. *Journal of Gastroenterology and Hepatology* **22**: 1959-64.
- Morales J, Perez-Tejada E, Montiel R (2008). Modificación superficial por plasma aplicada a biomateriales. In *La Física Biológica en México: Temas Selectos 2*, (Ed. Colegio Nacional, México), p. 195-205.
- Park JK, Lee DH (2005). Bioartificial liver systems: current status and future perspective. *Journal of Bioscience and Bioengineering* **99**: 311-319.
- Park J, Li Y, Berthiaume F, Toner M, Yarmush M L, Tilles A W (2008). Radial flow hepatocyte bioreactor using stacked microfabricated grooved substrates. *Biotechnology and Bioengineering* **99**: 455-467.
- Ramirez-Fernandez O, Godinez R, Morales J, Gomez-Quiroz L, Gutierrez-Ruiz MC, Zúñiga-Aguilar E, Olayo R (2012). Superficies modificadas mediante polimerización por plasma para cocultivos de modelos hepáticos. *Revista Mexicana de Ingeniería Biomedica* **33**: 6-12.
- Sherman M (2005). Hepatocellular carcinoma: epidemiology, risk factors, and screening. *Seminars in Liver Diseases* **25**: 143-154.
- Shi G, Rouabhia M, Wang Z, Dao L H, Zhang Z (2004). A novel electrically conductive and biodegradable composite made of polypyrrole nanoparticles and polylactide. *Biomaterials* **25**: 2477- 2488.
- Shoufeng Y, Kah-Fai L, Zhaohui D, Chee-Kai C (2001). The design of scaffolds for use in tissue engineering. Part I. Traditional factors. *Tissue Engineering* **7**: 679-689.
- Thomas RJ, Bennett A, Thomson B, Shakesheff KM (2006). Hepatic stellate cells on poly (DL- lactic acid) surfaces control the formation of 3D hepatocytes co-culture aggregates in vitro. *European Cells and Materials* **11**: 16-26.
- Wang X, Gu X, Yuan C, Chen S, Zhang P, Zhang T, Yao J, Chen F, Chen G (2004). Evaluation of biocompatibility of polypyrrole in vitro and in vivo. *Journal of Biomedical Material Research Part A* **68**: 411-422.
- Zhang Z, Roy R, Dugre FJ, Tessier D, Dao LH (2001). In vitro biocompatibility study of electrically conductive polypyrrole-coated polyester fabrics. *Journal of Biomedical Material Research Part A* **57**: 63-71.